Low-lying ^2S states of the singly charged carbon ion

István Hornyák,[1,*] Ludwik Adamowicz,[2,3,4,†] and Sergiy Bubin[1,‡]

[1]*Department of Physics, Nazarbayev University, Nur-Sultan 010000, Kazakhstan*

[2]*Department of Chemistry and Biochemistry, University of Arizona, Tucson, Arizona 85721, USA*

[3]*Department of Physics, University of Arizona, Tucson, Arizona 85721, USA*

[4]*Interdisciplinary Center for Modern Technologies, Nicolaus Copernicus University, ul. Wileńska 4, Toruń, PL 87-100, Poland*

(Received 1 September 2020; accepted 10 December 2020; published 30 December 2020)

In this work, we report benchmark variational calculations of the five lowest doublet S-states of the C^+ ion. The wave functions of this five-electron system are expanded in terms of 16 000 all-particle explicitly correlated Gaussians (ECGs) whose nonlinear variational parameters are subject to extensive optimization. The motion of the finite-mass nucleus is explicitly included in the Hamiltonian, while relativistic corrections to the energy levels are computed in the framework of the perturbation theory. Lowest-order quantum electrodynamics (QED) corrections are also estimated. The results obtained for the energy levels enable the determination of transition frequencies with the accuracy that approaches the available experimental data and may open up avenues for future determination of nuclear charge radii of carbon isotopes.

DOI: 10.1103/PhysRevA.102.062825

I. INTRODUCTION

Accurate energies and wave functions of few-electron atoms and molecules have been of considerable interest since the early days of quantum theory [1,2]. Nowadays, this interest stems primarily from two factors: The ongoing activity in the field of precision measurements motivated by the search for new physics beyond the Standard model and need for calibration data for the development of various *ab initio* methods that can effectively describe electronic correlations. Even at the nonrelativistic level of theory, one must resort to numerical approaches in order to obtain energy eigenvalues and the corresponding wave functions. Over the decades that have passed since the introduction of electronic computers in scientific research many different approaches have been developed for approximately solving the time-independent Schrödinger equation. In the case of few-electron atoms, the most accurate ones are mainly based on the use of the variational principle. The notion of what constitutes a high-precision numerical calculation certainly changed as computers became more capable and largely depends on the number of particles in the system. In variational calculations of atoms, the most effective approach is based on expanding the wave function of the system in terms of suitable basis functions that are capable of describing the short and long range behavior of the wave function and the electron correlation effects. It was demonstrated at the very beginning of computational atomic quantum mechanics that the basis functions explicitly dependent on the inter-electronic distances (the so-called explicitly correlated functions) are particularly effective in describing these effects. The early works of Hylleraas [1], Kinoshita [3], and Pekeris [4] on the helium atom initiated highly accurate studies of energy spectra of atoms that continue to this day.

While bound states of two- and three-electron atoms have been calculated with ultra-high accuracy using Hylleraas-type explicitly correlated functions (see, for example, works [5–10] and [11–13]), the approach involving this basis set has not been fully extended to atoms with four or more electrons due to difficulties with calculating the Hamiltonian matrix elements. There have been works on four-electron systems that involve the Hylleraas-type basis, but they utilized only a subset of that basis. King *et al.* [14] calculated the ground states of the Be I isoelectronic series using the Hylleraas approach with Slater-type basis functions, which contained at most one odd integer power in the r_{ij} factors. Sims and Hagstrom [15] used even more simplified Hy-CI basis. Another type of basis function that has been very popular in high-accuracy atomic calculations are explicitly correlated Gaussian functions (ECGs) [16–18]. These functions exponentially depend on squares of the interparticle distances. Powers of squares of the interparticle distance may also appear as pre-exponential multipliers. The most accurate results for four- and five-electron atoms have been obtained with ECGs [19–24]. These include the study of the ground state of the C^+ ion [19]. The largest atomic systems for which ECG calculations were performed include the neutral carbon and nitrogen atoms [17,25]. Due to the limited number of basis functions used in these calculations, however, the results are not yet as accurate as those for four- and five-electron systems.

The present high-accuracy calculations of the ^2S spectrum of the carbon cation, C^+, is a continuation of the development of capabilities to study increasingly larger atomic systems with high precision. Theoretical spectroscopy of carbon has relevance to astrophysics as this element is the fourth most abundant one in the universe and it is of fundamental importance in understanding the interstellar medium. Atomic

*Present address: ELTE Eötvös Loránd University, Institute of Chemistry,Pázmány Péter sétány 1/A, 1117 Budapest, Hungary; ihornyak@caesar.elte.hu

†ludwik@arizona.edu

‡sergiy.bubin@nu.edu.kz

carbon has been found in both neutral and ionic forms in many places in the interstellar medium [26–29].

The present study of the spectrum of the carbon cation also has relevance to its use in radiotherapy for cancer treatment. Particle therapy and, in particular, carbon ion therapy [30,31], which is a form of external beam radiotherapy, has been gaining prominence in recent years. In contrast to X-ray (photon beams) radiotherapy, carbon-ion beams exhibit a Bragg peak in energy loss when they cross the body. As a result, their maximum radiation dose can be delivered near the tumor minimizing damage to surrounding normal tissues [30,31]. Clinical studies have demonstrated advantages of the carbon-ion therapy in treating various forms of cancer, e.g., prostate, lung, liver, bone, etc. It is possible that using beams of excited carbon ions can further increase the effectiveness of the treatment.

II. METHOD

The approach used in this work to calculated the ^2S states of the C^+ ion was described in our previous papers [32]. Let us only briefly summarize the major feature of the method.

After separating the center-of-mass motion, the internal Hamiltonian used to determine internal bound states of the atom has the following form [32]:

$$H_{\rm nr} = -\frac{1}{2}\left(\sum_{i=1}^{5}\frac{1}{\mu_i}\nabla^2_{\mathbf{r}_i} + \sum_{i=1}^{5}\sum_{j\neq i}^{5}\frac{1}{m_0}\nabla'_{\mathbf{r}_i}\nabla_{\mathbf{r}_j}\right) + \sum_{i=1}^{5}\frac{q_0 q_i}{r_i} + \sum_{i=1}^{5}\sum_{j<i}^{5}\frac{q_i q_j}{r_{ij}}, \tag{1}$$

where q_i, $i = 1,\ldots,5$ are the electron charges, μ_i, $i = 1,\ldots,5$ are the reduced electron masses, $\mu_i \equiv m_0 m_i/(m_0 + m_i)$, where m_i, $i = 1,\ldots,5$ are the electron masses and m_0 is the mass of the nucleus located in the center of the coordinate system. $\mathbf{r}_i$, $i = 1,\ldots,5$ are the vectors pointing from the nucleus to the position of the ith electron and $r_{ij} = |\mathbf{r}_j - \mathbf{r}_i|$. $'$ stands for vector/matrix transpose. $q_0 = +6$ the charge of the carbon nucleus. In this work, we consider four isotopes of the carbon ion, namely, $^{12}C^+$, $^{13}C^+$, $^{14}C^+$, and $^{\infty}C^+$. The masses of the corresponding nuclei in atomic units are $m_0^{12} = 21\,868.663850$, $m_0^{13} = 23\,697.667827$, $m_0^{14} = 25,520.350606$, and $m_0^{\infty} = \infty$.

Hamiltonian (1) can also be conveniently written in the matrix form [17]:

$$H_{\rm nr} = -\nabla'_{\mathbf{r}}\mathbf{M}\nabla_{\mathbf{r}} + \sum_{i=1}^{5}\frac{q_0 q_i}{r_i} + \sum_{i=1}^{5}\sum_{j<i}^{5}\frac{q_i q_j}{r_{ij}}, \tag{2}$$

where

$$\nabla_{\mathbf{r}} = \begin{pmatrix}\nabla_{\mathbf{r}_1}\\ \vdots \\ \nabla_{\mathbf{r}_5}\end{pmatrix}$$

is a 15-component column gradient vector, and $\mathbf{M} = M \otimes I_3$ is the Kronecker product of a 5×5 matrix M and the 3×3 identity matrix I_3. The diagonal elements of matrix M are $1/(2\mu_1),\ldots,1/(2\mu_5)$, while all off-diagonal elements are equal to $1/(2m_0)$.

In order to obtain accurate eigenvalues and wave functions of the S states, we expand the wave functions in terms of all-electron explicitly correlated Gaussian (ECG) basis functions, which have the following form [17,18,33]:

$$\phi_k = \exp\left[-\mathbf{r}'(A_k \otimes I_3)\mathbf{r}\right]. \tag{3}$$

Here

$$\mathbf{r} = \begin{pmatrix}\mathbf{r}_1\\ \vdots \\ \mathbf{r}_5\end{pmatrix}$$

is a 15-component column vector of the internal coordinates and A_k is a 5×5 real symmetric positive definite matrix of adjustable parameters. Basis functions (3) are invariant under 3D rotations and, thus are eigenfunctions of the L^2 operator corresponding to zero total orbital angular momentum quantum number. It should be noted that matrix A_k is unique for each basis function. Its elements are determined through the variational minimization of the total nonrelativistic energy. In order to ensure the positive definiteness of A_k and avoid dealing with any constrains in the optimization process it is convenient to represent it in the Cholesky factorized form, $A_k = L_k L'_k$, where L_k is a real lower-triangular 5×5 matrix. The L_k matrix elements are the parameters that are variationally optimized in the calculation. The optimization is carried out with the aid of the analytical energy gradient determined with respect to the parameters. The proper permutation symmetry is implemented in the calculations using the spin-free formalism [34,35] as described, for example, in our previous work [32,36].

When accurate wave functions corresponding to the solution of the nonrelativistic problem are available, the most practical approach to account for small in magnitude relativistic and QED effects in light atoms is to use the perturbation theory. In this approach, the total energy can be expanded in powers of the fine structure constant, α [37,38]:

$$E_{\rm tot} = E_{\rm nr} + \alpha^2 E^{(2)}_{\rm rel} + \alpha^3 E^{(3)}_{\rm QED} + \alpha^4 E^{(4)}_{\rm HQED} + \cdots, \tag{4}$$

where $E_{\rm nr}$ is the nonrelativistic energy of the state being considered, the second term ($\alpha^2 E^{(2)}_{\rm rel}$) represents the leading relativistic corrections, the third term ($\alpha^3 E^{(3)}_{\rm QED}$) represents the leading QED corrections, and the fourth term ($\alpha^4 E^{(4)}_{\rm HQED}$) represent higher-order QED corrections, and so on. Each of these terms is evaluated as an expectation value of a certain operator.

Quantity $E^{(2)}_{\rm rel}$ corresponds to the expectation value of the Dirac–Breit Hamiltonian in the Pauli approximation, $H_{\rm rel}$ [39,40]. $H_{\rm rel}$ is transformed from the laboratory coordinates $\mathbf{R}_i$ to the internal coordinates $\mathbf{r}_i$ and for the S states includes what are known as the mass-velocity $H_{\rm MV}$, Darwin $H_{\rm D}$, orbit-orbit $H_{\rm OO}$, and spin-spin $H_{\rm SS}$ terms, respectively,

$$H_{\rm rel} = H_{\rm MV} + H_{\rm D} + H_{\rm OO} + H_{\rm SS}. \tag{5}$$

Their explicit forms in the internal coordinates are [17]

$$H_{\rm MV} = -\frac{1}{8}\left[\frac{1}{m_0^3}\left(\sum_{i=1}^{5}\nabla_{\mathbf{r}_i}\right)^4 + \sum_{i=1}^{5}\frac{1}{m_i^3}\nabla^4_{\mathbf{r}_i}\right], \tag{6}$$

$$H_{\rm D} = -\frac{\pi}{2}\left(\sum_{i=1}^{5}\frac{q_0 q_i}{m_i^2}\delta(\mathbf{r}_i) + \sum_{\substack{i,\,j=1\\ j\neq i}}^{5}\frac{q_i q_j}{m_i^2}\delta(\mathbf{r}_{ij})\right), \tag{7}$$

$$\begin{aligned} H_{\rm OO} = &-\frac{1}{2}\sum_{i=1}^{5}\frac{q_0 q_i}{m_0 m_i}\left(\frac{1}{r_i}\nabla'_{\mathbf{r}_i}\nabla_{\mathbf{r}_i} + \frac{1}{r_i^3}\mathbf{r}'_i(\mathbf{r}'_i\nabla_{\mathbf{r}_i})\nabla_{\mathbf{r}_i}\right)\\ &-\frac{1}{2}\sum_{\substack{i,\,j=1\\ j\neq i}}^{5}\frac{q_0 q_i}{m_0 m_i}\left(\frac{1}{r_i}\nabla'_{\mathbf{r}_i}\nabla_{\mathbf{r}_j} + \frac{1}{r_i^3}\mathbf{r}'_i(\mathbf{r}'_i\nabla_{\mathbf{r}_i})\nabla_{\mathbf{r}_j}\right)\\ &+\frac{1}{2}\sum_{\substack{i,\,j=1\\ j>i}}^{5}\frac{q_i q_j}{m_i m_j}\left(\frac{1}{r_{ij}}\nabla'_{\mathbf{r}_i}\nabla_{\mathbf{r}_j} + \frac{1}{r_{ij}^3}\mathbf{r}'_{ij}\left(\mathbf{r}'_{ij}\nabla_{\mathbf{r}_i}\right)\nabla_{\mathbf{r}_j}\right), \end{aligned} \tag{8}$$

and

$$H_{\rm SS} = -\frac{8\pi}{3}\sum_{\substack{i,\,j=1\\ j>i}}^{5}\frac{q_i q_j}{m_i m_j}(\mathbf{s}'_i\mathbf{s}_j)\delta(\mathbf{r}_{ij}). \tag{9}$$

In the above formulas $\delta(\ldots)$ is the three-dimensional Dirac delta function and $\mathbf{s}_i$ are spin operators for individual electrons. For all states considered in this work, $\mathbf{s}'_i\mathbf{s}_j = -3/4$. It should be noted that $E^{(2)}_{\rm rel}$ effectively contains both nonrecoil and recoil contributions if the nonrelativistic variational wave function used in the calculation of the expectation values of the relativistic and QED operators is generated using a finite mass of the nucleus in the nonrelativistic Hamiltonian.

Quantity $E^{(3)}_{\rm QED}$ represents the leading QED correction. For an atomic system, it accounts for the two-photon exchange, the vacuum polarization, and the electron self-energy effects. The explicit form of the corresponding operator is

$$\begin{aligned} H_{\rm QED} = &\sum_{\substack{i,\,j=1\\ j>i}}^{5}\left[\left(\frac{164}{15} + \frac{14}{3}\ln\alpha\right)\delta(\mathbf{r}_{ij}) - \frac{7}{6\pi}\mathcal{P}\left(\frac{1}{r_{ij}^3}\right)\right]\\ &+\sum_{i=1}^{5}\left(\frac{19}{30} - 2\ln\alpha - \ln k_0\right)\frac{4q_0}{3}\delta(\mathbf{r}_i), \end{aligned} \tag{10}$$

where the first sum represents the Araki-Sucher term [41–45], while the expectation value of $\mathcal{P}(1/r_{ij}^3)$ is defined as

$$\left\langle\mathcal{P}\left(\frac{1}{r_{ij}^3}\right)\right\rangle = \lim_{a\to 0}\left\langle\frac{1}{r_{ij}^3}\Theta(r_{ij}-a) + 4\pi(\gamma+\ln a)\delta(\mathbf{r}_{ij})\right\rangle. \tag{11}$$

In the last expression, Θ is the Heaviside step function and $\gamma = 0.577215\ldots$ is the Euler–Mascheroni constant.

Expression (10) also contains a term that includes the so-called Bethe logarithm, $\ln k_0$. This term represents the dominant part of the electron self-energy. Accurate calculation of this quantity for multielectron systems still represents a major difficulty. However, it is known that the dominant contribution to $\ln k_0$ comes from the inner shell electrons. This was first demonstrated by Drake and Goldman [46] and stated explicitly by Yan *et al.* [47]. The latter paper presented results for Be^+ and Li that can be extrapolated to C^+. The paper also showed the Bethe logarithm is not just approximately independent of the state, but also of the nuclear charge and the ionization stage of the atom. The approximate invariance of the Bethe logarithm becomes more apparent upon subtraction of $\ln(Z^2)$ as in this case it becomes close to the 2.984128556...value for the $1s$ electron [46].

TABLE I. Approximate values of the Bethe logarithm used in the calculations of the QED corrections for the lowest five ^2S states of C^+. All values are in atomic units.

State no.	Dominant configuration	$\ln k_0$	$\ln(k_0/Z^2)$
1	$1s^2 2s 2p^2\ (^2S)$	6.5598	2.9763
2	$1s^2 2s^2 3s\ (^2S)$	6.5574	2.9739
3	$1s^2 2s^2 4s\ (^2S)$	6.5574	2.9739
4	$1s^2 2s^2 5s\ (^2S)$	6.5574	2.9739
5	$1s^2 2s^2 6s\ (^2S)$	6.5574	2.9739

Therefore, at the lowest level of approximation, one can use the Bethe logarithm values for the C^{4+} or C^{2+} ions. The former is known to high accuracy [9] and is equal to 6.566235886(1) a.u. The latter was computed in work [48] for the two lowest singlet S-states with dominant electronic configurations $1s^2 2s^2$ and $1s^2 2p^2$. The corresponding values are 6.5574(4) and 6.5642(8) a.u. Table I lists the values of the Bethe logarithm, which we adopted for each of the states of C^+ considered in this work. We approximated the values of the Bethe logarithm (β) based on the number of $2s$ (n_{2s}) and $2p$ (n_{2p}) electrons in the dominant configuration of each state by means of the following linear expression:

$$\beta = \beta_{1s^2} + [\beta_{1s^2 2s^2} - \beta_{1s^2}]\frac{n_{2s}}{2} + [\beta_{1s^2 2p^2)} - \beta_{1s^2}]\frac{n_{2p}}{2}.$$

For the lowest state, which corresponds to configuration $1s^2 2s 2p^2$, it gives the value of 6.5598 a.u.

The last term in (4), $E^{(4)}_{\rm HQED}$, is computed as an expectation value of the following approximate operator derived by Pachucki *et al.* [49,50]:

$$H_{\rm HQED} = \pi q_0^2\left(\frac{427}{96} - 2\ln 2\right)\sum_{i=1}^{5}\delta(\mathbf{r}_i). \tag{12}$$

$E^{(4)}_{\rm HQED}$ includes the dominating electron-nucleus one-loop radiative correction and neglects the two-loop radiative correction, electron-electron radiative correction, and the higher-order relativistic corrections.

It should be mentioned that Eq. (12) was previously proposed and used by Drake and Martin [51] and it is a simple generalization of the Kabir–Salpeter formula [43] for two electrons applied to the five-electron Lamb shift (also, see the work of Ermolaev [52] for additional insight on the matter). Based on the data available for smaller atoms one can expect that Eq. (12) should capture the bulk of the higher-order QED effects with the overall error being less than 50%.

It should be noted that the expectation values of both $H_{\rm QED}$ and $H_{\rm HQED}$ Hamiltonians are calculated with the infinite nuclear mass wave functions, because the underlying formalism in the first approximation was been developed under the assumption of a clamped nucleus. Hence, no

TABLE II. Some key expectation values (all in atomic units) for the five lowest ^2S states of $^{12}C^+$, $^{13}C^+$, $^{14}C^+$, and $^{\infty}C^+$ ions computed with the largest basis sets of 16 000 ECG functions used in this work. The tilde sign indicates that the regularization technique was used to compute the expectation value. The numbers in parentheses are estimated uncertainties due to the basis truncation.

State	Isotope	$\langle\tilde{H}_{\rm MV}\rangle$	$\langle\tilde{\delta}(\mathbf{r}_i)\rangle$	$\langle\tilde{\delta}(\mathbf{r}_{ij})\rangle$	$\langle H_{\rm OO}\rangle$	$\langle\mathcal{P}(1/r_{ij}^3)\rangle$
$2s2p^2$	$^{12}C^+$	−1461.2153(5)	25.109474(3)	0.6503804(3)	−0.062781(1)	
	$^{13}C^+$	−1461.2368(5)	25.109753(3)	0.6503867(3)	−0.054542(1)	
	$^{14}C^+$	−1461.2551(5)	25.109991(3)	0.6503921(3)	−0.047506(1)	
	$^{\infty}C^+$	−1461.4932(5)	25.113086(3)	0.6504620(3)	0.043986(1)	−6.6842(50)
$2s^23s$	$^{12}C^+$	−1511.4368(2)	25.912321(4)	0.6763524(3)	−2.251523(4)	
	$^{13}C^+$	−1511.4580(2)	25.912592(4)	0.6763585(3)	−2.242852(4)	
	$^{14}C^+$	−1511.4761(2)	25.912823(4)	0.6763636(3)	−2.235447(4)	
	$^{\infty}C^+$	−1511.7117(2)	25.915830(4)	0.6764310(3)	−2.139159(4)	−7.4489(30)
$2s^24s$	$^{12}C^+$	−1511.5693(2)	25.921466(3)	0.6758074(2)	−2.395628(2)	
	$^{13}C^+$	−1511.5909(2)	25.921744(3)	0.6758137(2)	−2.386976(2)	
	$^{14}C^+$	−1511.6094(2)	25.921982(3)	0.6758190(2)	−2.379587(2)	
	$^{\infty}C^+$	−1511.8501(2)	25.925070(3)	0.6758889(2)	−2.283510(2)	−7.5038(20)
$2s^25s$	$^{12}C^+$	−1510.6305(5)	25.908809(5)	0.6752095(4)	−2.393486(4)	
	$^{13}C^+$	−1510.6522(5)	25.909087(5)	0.6752158(4)	−2.384841(4)	
	$^{14}C^+$	−1510.6707(5)	25.909325(5)	0.6752212(4)	−2.377457(4)	
	$^{\infty}C^+$	−1510.9112(5)	25.912412(5)	0.6752910(4)	−2.281451(4)	−7.5069(50)
$2s^26s$	$^{12}C^+$	−1510.2470(10)	25.903643(15)	0.6749708(10)	−2.391852(12)	
	$^{13}C^+$	−1510.2687(10)	25.903921(15)	0.6749771(10)	−2.383209(12)	
	$^{14}C^+$	−1510.2872(10)	25.904158(15)	0.6749824(10)	−2.375828(12)	
	$^{\infty}C^+$	−1510.5277(10)	25.907247(15)	0.6750523(10)	−2.279848(12)	−7.5122(100)

recoil effects are included in $E^{(3)}_{\rm QED}$ and $E^{(4)}_{\rm HQED}$ computed in this work. However, it should be noted that the finite-mass corrections to the lowest-order QED corrections (radiative recoil) are well known from the works of Pachucki and Sapirstein [53] and Yan and Drake [54] and could be included within the conventional approach where the zero-order approximation is obtained from an infinite-mass nonrelativistic calculation.

Operators (6), (7), (9), (10), and (12) contain singular terms [e.g., $\delta(\mathbf{r}_{ij})$], whose expectation values are known to converge rather slowly with increasing the length of the basis used to expand the wave function. The primary reason for this is that when these expectation values are computed, the approximate variational wave function $\psi_{\rm appr}$ is sampled locally (in a subspace) rather than globally. The accuracy of the final result then depends on the residual value, $\epsilon\delta\psi = \psi - \psi_{\rm appr}$, averaged in the subspace (here $\delta\psi$ is a normalized function and ϵ is a parameter that becomes small when $\psi_{\rm appr} \to \psi$, with ψ being the exact wave function) and may behave as $\mathcal{O}(\epsilon)$. At the same time, the error in the energy in the variational method behaves as $\mathcal{O}(\epsilon^2)$. Thus the number of converged figures in the expectation values of singular operators can be twice fewer than in the nonrelativistic energy. This behavior is general and occurs in the case of any basis set employed. On top of that, Gaussian basis functions (3) have improper behavior in the vicinity of particle coalescence points and their linear combinations cannot satisfy the Kato cusp conditions [55]. While it does not render them unusable for variational calculations, it does cause an additional slow down in the convergence of the expectation values of $\delta(\mathbf{r}_{ij})$ and some other singular operators. In order to overcome these issues, we employed a regularization technique implemented in the spirit of works [56,57]. For the expectation values of the delta functions, we employ the following Drachman identities in the internal coordinates:

$$\langle\psi|\delta(\mathbf{r}_i)|\psi\rangle = \frac{\mu_i}{\pi}\left[\left\langle\psi\left|\frac{E-V}{r_i}\right|\psi\right\rangle - \left\langle\nabla_{\mathbf{r}}\psi\left|\frac{\mathbf{M}}{r_i}\right|\nabla_{\mathbf{r}}\psi\right\rangle\right], \tag{13}$$

$$\langle\psi|\delta(\mathbf{r}_{ij})|\psi\rangle = \frac{\mu_{ij}}{\pi}\left[\left\langle\psi\left|\frac{E-V}{r_i}\right|\psi\right\rangle - \left\langle\nabla_{\mathbf{r}}\psi\left|\frac{\mathbf{M}}{r_{ij}}\right|\nabla_{\mathbf{r}}\psi\right\rangle\right]. \tag{14}$$

In the above expressions, $\mu_{ij} \equiv m_i m_j/(m_i+m_j)$, V is the potential energy operator, and E is the variational energy. The identities hold for the exact wave function, ψ. When the wave function is approximated by a linear combination with a progressively larger number of expansion terms, the right hand sides of expressions (13) and (14) converge to the corresponding exact limits much faster than the unregularized series because they do not contain any singular operators.

The presence of the fourth power of linear momenta in $H_{\rm MV}$ [Eq. (6)] also causes slow convergence of the corresponding expectation values. To remedy this, $H_{\rm MV}$ can be written in the matrix form as

$$H_{\rm MV} = -(\nabla'_{\mathbf{r}}\beta_0\mathbf{J}\nabla_{\mathbf{r}})^2 - \sum_{i=1}^{5}(\nabla'_{\mathbf{r}}\beta_i\mathbf{J}_{ii}\nabla_{\mathbf{r}})^2, \tag{15}$$

where $\beta_0 = 1/\sqrt{8m_0^3}$, $\beta_i = 1/\sqrt{8m_i^3}$, $\mathbf{J} = (J\otimes I_3)$, $\mathbf{J}_{ii} = J_{ii}\otimes I_3 J$ is a 5×5 matrix with all its elements equal to 1, and J_{ii} is a 5×5 matrix that has only a single nonzero element, $(J_{ii})_{ii} = 1$.

For $H_{\rm MV}$, we use the identity

$$\langle\psi|H_{\rm MV}|\psi\rangle = -\lambda^2\langle\psi|(E-V)^2|\psi\rangle - \lambda^2\langle\psi|(E-V)(\nabla'_{\mathbf{r}}\mathbf{B}\nabla_{\mathbf{r}})|\psi\rangle$$

TABLE III. Nonrelativistic and total energies computed with the largest basis sets of 16 000 ECGs along with their extrapolated values. All energies are in atomic units.

State	Isotope	Basis	$E_{\rm nr}$	$E_{\rm tot}$
$2s2p^2$	$^{12}C^+$	16 000	−36.99019765	−37.00228427
		∞	−36.99019791(15)	−37.00228451(15)
	$^{13}C^+$	16 000	−36.99032676	−37.00241337
		∞	−36.99032702(15)	−37.00241361(15)
	$^{14}C^+$	16 000	−36.99043702	−37.00252362
		∞	−36.99043727(15)	−37.00252386(15)
	$^{\infty}C^+$	16 000	−36.99187059	−37.00395712
		∞	−36.99187084(15)	−37.00395736(15)
$2s^23s$	$^{12}C^+$	16 000	−36.89819206	−36.91095784
		∞	−36.89819216(6)	−36.91095793(6)
	$^{13}C^+$	16 000	−36.89832441	−36.91109016
		∞	−36.89832450(6)	−36.91109026(6)
	$^{14}C^+$	16 000	−36.89843742	−36.91120316
		∞	−36.89843752(6)	−36.91120325(6)
	$^{\infty}C^+$	16 000	−36.89990687	−36.91267237
		∞	−36.89990697(6)	−36.91267246(6)
$2s^24s$	$^{12}C^+$	16 000	−36.71277198	−36.72552973
		∞	−36.71277208(7)	−36.72552984(7)
	$^{13}C^+$	16 000	−36.71290407	−36.72566181
		∞	−36.71290417(7)	−36.72566192(7)
	$^{14}C^+$	16 000	−36.71301688	−36.72577461
		∞	−36.71301698(7)	−36.72577471(7)
	$^{\infty}C^+$	16 000	−36.71448359	−36.72724115
		∞	−36.71448369(7)	−36.72724126(7)
$2s^25s$	$^{12}C^+$	16 000	−36.63936599	−36.65210721
		∞	−36.63936624(16)	−36.65210745(16)
	$^{13}C^+$	16 000	−36.63949782	−36.65223902
		∞	−36.63949807(16)	−36.65223926(16)
	$^{14}C^+$	16 000	−36.63961039	−36.65235158
		∞	−36.63961064(16)	−36.65235182(16)
	$^{\infty}C^+$	16 000	−36.64107412	−36.65381514
		∞	−36.64107437(16)	−36.65381538(16)
$2s^26s$	$^{12}C^+$	16 000	−36.60330234	−36.61603673
		∞	−36.60330306(47)	−36.61603745(47)
	$^{13}C^+$	16 000	−36.60343403	−36.61616841
		∞	−36.60343475(47)	−36.61616913(47)
	$^{14}C^+$	16 000	−36.60354649	−36.61628085
		∞	−36.60354721(47)	−36.61628157(47)
	$^{\infty}C^+$	16 000	−36.60500870	−36.61774290
		∞	−36.60500942(47)	−36.61774362(47)

$$+\lambda^2\langle\psi|(\nabla'_{\mathbf{r}}\mathbf{M}\nabla_{\mathbf{r}})^2|\psi\rangle+\lambda^2\langle\psi|(\nabla'_{\mathbf{r}}\mathbf{M}\nabla_{\mathbf{r}})(\nabla'_{\mathbf{r}}\mathbf{B}\nabla_{\mathbf{r}})|\psi\rangle$$
$$-\beta_0\langle\psi|(\nabla'_{\mathbf{r}}\mathbf{J}\nabla_{\mathbf{r}})^2|\psi\rangle-\sum_{i=1}^{n}\beta_i\langle\psi|(\nabla'_{\mathbf{r}}\mathbf{J}_{ii}\nabla_{\mathbf{r}})^2|\psi\rangle. \quad (16)$$

Parameter λ and matrix $\mathbf{B}=B\otimes I_3$ in this identity are chosen such that the element(s) of the diagonal matrix B corresponding to the lightest particle(s) in the system vanish. Namely, if particle k is the lightest one (in the present case it is an electron), we adopt

$$\lambda^2=\frac{\beta_0^2+\beta_k^2}{(M)_{kk}^2}, \quad (17)$$

and then the elements of B are

$$(B)_{ii}=\frac{\beta_0^2+\beta_k^2}{\lambda^2(M)_{ii}}-(M)_{ii}. \quad (18)$$

When the difference between the lightest mass, m_k, and the masses of other particles in the system (in our case m_0) is very large, the right-hand side of expression (16) converges to the exact limit considerably faster upon increasing the basis size.

III. RESULTS

The numerical value of the conversion factor from Hartrees to wave numbers used in present work is 1 Hartree = $2.194\,746\,313\,702\times10^5$ cm^{-1} [58]. The value of the fine structure constant used in the calculations of the relativistic and QED corrections to the total energy is $\alpha=7.297\,352\,5664\times10^{-3}$ [58].

The present calculations concern the five lowest ^{2}S states of the three isotopes of the carbon cation, i.e., $^{12}C^+$, $^{13}C^+$, and $^{14}C^+$, as well as the carbon cation with an infinite nuclear mass, $^{\infty}C^+$. The basis set optimization is performed for each of the five states of the main isotope, $^{12}C^+$, and then reused in the calculations for the corresponding states of the other two isotopes and for $^{\infty}C^+$. Thus, the relatively small change of the wave function due to the change of the nuclear mass is only described through the adjustment of the linear expansion coefficients of the basis functions. Such an approach has been found sufficient in our previous atomic calculations [36].

Generating the basis set for the lowest-energy state is initiated with a small set of randomly selected Gaussians and involves variational reoptimization of their nonlinear exponential parameters using a scheme that employs the analytically calculated gradient of the energy of the state with respect to the parameters. Next, the basis set is enlarged by an addition of some fixed number of functions (usually from 20 to 100). The functions are added one by one. The initial guess for an added function is obtained by taking a subset of functions already included in the basis set that give the largest contribution to the energy of the state, randomly perturbing their nonlinear parameters, and selecting the function that lowers the energy the most. Next, the nonlinear parameters of the selected function are optimized and, if the function after the optimization is not linearly dependent with other functions in the basis set, the function is added to the set. After a certain number of functions are added to the basis set, the whole set is reoptimized. After a fairly good set of functions is generated for the lowest-energy state, the set is used as an initial basis set for the next state and, after its reoptimization for that state, it is used as the initial basis set for the following state, etc. The basis sets for all five considered states of $^{12}C^+$ are enlarged to the size of 16 000 functions. At that point several additional optimization cycles are performed for each set. At the final stages of basis growing and optimization we use the so-called extended computer precision (80-bit per number; about 19 decimal figures of precision) as it increased the numerical accuracy of the calculations and allows to noticeably accelerate the energy convergence.

The results presented next (in tables) are limited to the values obtained using the largest basis sets of 16 000 Gaussians. The values obtained with smaller basis sets are used to

TABLE IV. Transition energies, ΔE (in cm^{-1}), between adjacent ^2S states of the $^{12}C^+$, $^{13}C^+$ and $^{14}C^+$ ions computed using infinite nuclear mass (INM,i) nonrelativistic energies, and then gradually corrected by including finite nuclear mass (FNM,f), relativistic, and QED effects. As the QED and HQED Hamiltonians are only valid for INM, the corresponding energy corrections are computed using the wave functions obtained in INM calculations. The estimated uncertainties shown for the extrapolated transition energies are due to the basis truncation.

Isotope	Contributions included in ΔE	Basis size	$2s2p^2 \leftarrow 2s^23s$	$2s^23s \leftarrow 2s^24s$	$2s^24s \leftarrow 2s^25s$	$2s^25s \leftarrow 2s^26s$
$^{12}C^+$	nr(i)	16 000	20 183.70	40 695.71	16 111.52	7915.44
	nr(f)	16 000	20 192.89	40 695.01	16 110.75	7915.06
	nr(f)+rel(f)	16 000	20 032.06	40 696.61	16 114.56	7916.62
	nr(f)+rel(f)+QED(i)	16 000	20 042.97	40 696.76	16 114.40	7916.56
	nr(f)+rel(f)+QED(i)+HQED(i)	16 000	20 043.83	40 696.77	16 114.38	7916.55
	nr(f)+rel(f)+QED(i)+HQED(i)	∞	20 043.88(5)	40 696.77(1)	16 114.34(4)	7916.45(10)
	Experiment, NIST ASD [59]		20 043.91(1)	40 696.42(1)	16 113.77(1)	7916.40 (1)
$^{13}C^+$	nr(i)	16 000	20 183.70	40 695.71	16 111.52	7915.44
	nr(f)	16 000	20 192.18	40 695.06	16 110.81	7915.09
	nr(f)+rel(f)	16 000	20 031.36	40 696.66	16 114.62	7916.65
	nr(f)+rel(f)+QED(i)	16 000	20 042.26	40 696.81	16 114.46	7916.59
	nr(f)+rel(f)+QED(i)+HQED(i)	16 000	20 043.13	40 696.82	16 114.44	7916.58
	nr(f)+rel(f)+QED(i)+HQED(i)	∞	20 043.18(5)	40 696.82(1)	16 114.40 (4)	7916.48(10)
$^{14}C^+$	nr(i)	16 000	20 183.70	40 695.71	16 111.52	7915.44
	nr(f)	16 000	20 191.58	40 695.11	16 110.86	7915.11
	nr(f)+rel(f)	16 000	20 030.75	40 696.71	16 114.67	7916.68
	nr(f)+rel(f)+QED(i)	16 000	20 041.66	40 696.85	16 114.51	7916.62
	nr(f)+rel(f)+QED(i)+HQED(i)	16 000	20 042.53	40 696.86	16 114.49	7916.61
	nr(f)+rel(f)+QED(i)+HQED(i)	∞	20 042.58(5)	40 696.86(1)	16 114.45(4)	7916.51(10)

extrapolate the results to an infinite number of basis functions and to estimate their uncertainties. First, we discuss the data shown in Tables II and III. The data in Table II concern expectation values of the operators involved in the expressions for the leading relativistic correction and the leading QED corrections. Three of the quantities shown in the table, namely, $\langle \tilde{H}_{\mathrm{MV}} \rangle$, $\langle \tilde{\delta}(\mathbf{r}_i) \rangle$, and $\langle \tilde{\delta}(\mathbf{r}_{ij}) \rangle$, are calculated using the regularization procedure described in Section II, while the other two quantities, i.e., $\langle H_{\mathrm{OO}} \rangle$ and $\langle \mathcal{P}(1/r_{ij}^3) \rangle$, are computed directly without regularization. The quantities are calculated for the three carbon cation isotopes and for $^{\infty}C^+$ for all five considered states. An estimated uncertainty due to basis incompleteness is shown for each quantity. In Table III, we show the total nonrelativistic energies calculated for the five states of all isotopes and the total energies that include the corresponding relativistic and QED corrections (E_{nr} and E_{tot}) calculated using the quantities from Table II. Besides the energies obtained with 16 000 basis functions, the energies extrapolated to the basis set limit are also shown along with their estimated uncertainties.

In general, the quantities presented in Tables II and III show monotonic behavior in terms of increasing the nuclear mass (from ^{12}C to $^{\infty}C$) and in terms of increasing the level of the electronic excitation of the system. The mass effects are pronounced and their contribution vary from affecting the fifth significant figure in the results for $\langle \tilde{H}_{\mathrm{MV}} \rangle$ and the two delta functions to affecting the first significant figure in the results for $\langle H_{\mathrm{OO}} \rangle$. The latter quantity shows some interesting behavior with respect to the level of the electronic excitation. While the $\langle H_{\mathrm{OO}} \rangle$ values for the second, third, fourth, and fifth states lie in the range from -2.1 to -2.4 a.u., the value for the first, lowest-energy state is about 4–5 times lower and for infinite nuclear mass it is positive. Clearly, this is a result of the configurational composition of the wave functions of the states. While, the former states are conventional Rydberg-type excitations with the valence electron being successively promoted from the $3s$ orbital to the ns orbital (with $n = 4,\ 5$, and 6), for the first state the dominant configuration is $1s^22s2p^2$. In that configuration one valence electron occupies the $2s$ orbital and two valence electrons occupies two different p orbitals. That makes the orbit-orbit interactions between the electrons significantly smaller for the lowest-energy state than for the other states.

The quantities from Tables II and III are used to calculate the transition energies between adjacent states. These energies are shown in Table IV, where all values are given in cm^{-1}. The transition energies are calculated using the results obtained with 16 000 ECGs. The values obtained by extrapolating to the basis set limits are also shown in the table. For each transition and for each carbon isotope, the contributions to the transition energy are shown starting from the nonrelativistic infinite-nuclear-mass value and then successively including the contributions due the finite-nuclear-mass effects, relativistic corrections, and QED effects. For the lowest $2s2p^2 \leftarrow 2s^23s$ transition, the FNM-effect contribution amounts to about 9 cm^{-1}, but the contribution decreases to less than 1 cm^{-1} for the other transitions. The infinite-nuclear-mass contribution is calculated from the total nonrelativistic energies obtained from the $^{\infty}C^+$ calculations and the finite-nuclear-mass contribution is obtained by subtracting the infinite-nuclear-mass nonrelativistic transition energy from the finite-nuclear-mass nonrelativistic transition energy. By far the largest of all additional contributions is the contribution due to the relativistic effects. For the lowest transition this contribution is about -150 cm^{-1}, but it significantly decreases for the other transitions. For the $2s^25s \leftarrow 2s^26s$ transition it is only about 1.5 cm^{-1}. The leading QED effects contribute to the lowest transition energy by about

TABLE V. Expectation values of powers of the interparticle distances, $\langle r_i^p \rangle$ and $\langle r_{ij}^p \rangle$ ($p = -2, \ldots, 2$), computed with the largest basis sets of 16 000 ECG functions used in this work. All values are in atomic units.

State	Isotope	$\langle r_i^{-2} \rangle$	$\langle r_{ij}^{-2} \rangle$	$\langle r_i^{-1} \rangle$	$\langle r_{ij}^{-1} \rangle$	$\langle r_i \rangle$	$\langle r_{ij} \rangle$	$\langle r_i^2 \rangle$	$\langle r_{ij}^2 \rangle$
$2s2p^2$	$^{12}C^+$	27.319692(3)	2.728177(2)	2.7977255(1)	0.9951368(0)	1.054674(0)	1.724375(0)	1.967321(1)	4.075430(2)
	$^{13}C^+$	27.319894(3)	2.728191(2)	2.7977345(1)	0.9951381(0)	1.054674(0)	1.724377(0)	1.967331(1)	4.075449(2)
	$^{14}C^+$	27.320065(3)	2.728202(2)	2.7977422(1)	0.9951392(0)	1.054675(0)	1.724378(0)	1.967339(1)	4.075465(2)
	$^{\infty}C^+$	27.322300(3)	2.728355(2)	2.7978425(1)	0.9951534(0)	1.054680(0)	1.724399(0)	1.967446(1)	4.075672(2)
$2s^23s$	$^{12}C^+$	27.893464(3)	2.603788(2)	2.7518376(1)	0.8758744(3)	1.455866(1)	2.498558(2)	4.661907(5)	9.633307(10)
	$^{13}C^+$	27.893658(3)	2.603805(2)	2.7518477(1)	0.8758782(3)	1.455858(1)	2.498544(2)	4.661856(5)	9.633205(10)
	$^{14}C^+$	27.893824(3)	2.603819(2)	2.7518563(1)	0.8758814(3)	1.455851(1)	2.498532(2)	4.661811(5)	9.633119(10)
	$^{\infty}C^+$	27.895985(3)	2.604009(2)	2.7519684(1)	0.8759238(3)	1.455761(1)	2.498377(2)	4.661238(5)	9.631992(10)
$2s^24s$	$^{12}C^+$	27.875852(3)	2.558729(1)	2.7192474(1)	0.8151880(1)	2.327263(2)	4.201103(5)	16.76223(2)	33.72007(5)
	$^{13}C^+$	27.876052(3)	2.558745(1)	2.7192571(1)	0.8151906(1)	2.327255(2)	4.201088(5)	16.76210(2)	33.71983(5)
	$^{14}C^+$	27.876222(3)	2.558758(1)	2.7192654(1)	0.8151928(1)	2.327248(2)	4.201075(5)	16.76200(2)	33.71962(5)
	$^{\infty}C^+$	27.878441(3)	2.558932(1)	2.7193729(1)	0.8152219(1)	2.327155(2)	4.200907(5)	16.76064(2)	33.71692(5)
$2s^25s$	$^{12}C^+$	27.859356(5)	2.548749(3)	2.7067644(1)	0.7924201(1)	3.476398(20)	6.486172(40)	45.74634(50)	91.65383(100)
	$^{13}C^+$	27.859556(5)	2.548765(3)	2.7067740(1)	0.7924226(1)	3.476386(20)	6.486150(40)	45.74603(50)	91.65321(100)
	$^{14}C^+$	27.859727(5)	2.548778(3)	2.7067823(1)	0.7924247(1)	3.476376(20)	6.486131(40)	45.74576(50)	91.65267(100)
	$^{\infty}C^+$	27.861945(5)	2.548951(3)	2.7068891(1)	0.7924526(1)	3.476246(20)	6.485889(40)	45.74227(50)	91.64570(100)
$2s^26s$	$^{12}C^+$	27.852724(10)	2.544884(10)	2.7004194(3)	0.7805979(7)	4.922314(200)	9.371746(300)	103.1373(50)	206.4175(200)
	$^{13}C^+$	27.852924(10)	2.544899(10)	2.7004290(3)	0.7806003(7)	4.922301(200)	9.371722(300)	103.1367(50)	206.4163(200)
	$^{14}C^+$	27.853095(10)	2.544913(10)	2.7004372(3)	0.7806024(7)	4.922290(200)	9.371702(300)	103.1363(50)	206.4154(200)
	$^{\infty}C^+$	27.855314(10)	2.545085(10)	2.7005436(3)	0.7806293(7)	4.922149(200)	9.371437(300)	103.1300(50)	206.4028(200)

11 cm^{-1}, but this contribution also significantly decreases to below 0.2 cm^{-1} for the $2s^23s \leftarrow 2s^24s$ transition and to 0.06 for the $2s^25s \leftarrow 2s^26s$ transition. The estimated contribution from the higher-order QED effects is below 1 cm^{-1} for the lowest transition and also significantly decreases for the transitions between higher states.

The results shown in Table IV allow for an estimation of the isotopic effects in the transition energies. Using the transition energies obtained with 16 000 basis functions at the highest level of the theory, i.e., the nonrel + rel + QED + HQED level, the isotopic shift for the lowest $1^2S \leftarrow 2^2S$ transition in going from $^{12}C^+$ to $^{13}C^+$ amounts to about -0.7 cm^{-1} and to about -0.6 cm^{-1} in going from $^{13}C^+$ to $^{14}C^+$ (i.e., the transition energy decreases in this case). The isotopic shift is much smaller for the $2s^25s \leftarrow 2s^26s$ transition, but it has the opposite sign (+0.03 cm^{-1}). Finally, the calculated transitions for the $^{12}C^+$ isotope can be compared with the experimental values. The comparison is shown in Table IV. Let us consider the results obtained at the highest level of theory (without the extrapolation to the basis set limit). For the lowest $2s2p^2 \leftarrow 2s^23s$ transition, our calculated value of 20 043.83 cm^{-1} is very close to the experimental result, deviating by only 0.08 cm^{-1}. For the $2s^23s \leftarrow 2s^24s$ transition, the calculated value is 40 696.77 cm^{-1} and the experiment gives 40 696.42 cm^{-1}. For the last two transitions, i.e., $2s^24s \leftarrow 2s^25s$ and $2s^25s \leftarrow 2s^26s$, the calculated values vs. the experimental values are: 16 114.38 and 7916.55 cm^{-1}, and 16 113.77 and 7916.40 cm^{-1}, respectively. Our calculated transition energies for the lowest and higher transitions agree with the experimental values within the uncertainty due to the basis-set truncation. For the other two transitions, the discrepancy is small, about 0.1–0.6 cm^{-1}, yet well outside of both the experimental and numerical error bar. The exact origin of this discrepancy is not immediately clear. It may come from the approximate treatment of the HQED correction in our calculations or from even higher order QED corrections missing in our model. It is also possible that actual accuracy of the experimentally derived transition energies in the NIST database is lower than the quoted value of 0.01 cm^{-1}.

In the last table, Table V, the expectation values of some positive and negative powers of the electron-nucleus distance r_i and the electron-electron distance r_{ij} are shown for all considered states and for all considered isotopes including $^{\infty}C^+$. By looking at this data one can compare the isotopic shifts of the $\langle r_i \rangle$ and $\langle r_{ij} \rangle$ expectation values for the lowest $2s2p^2$

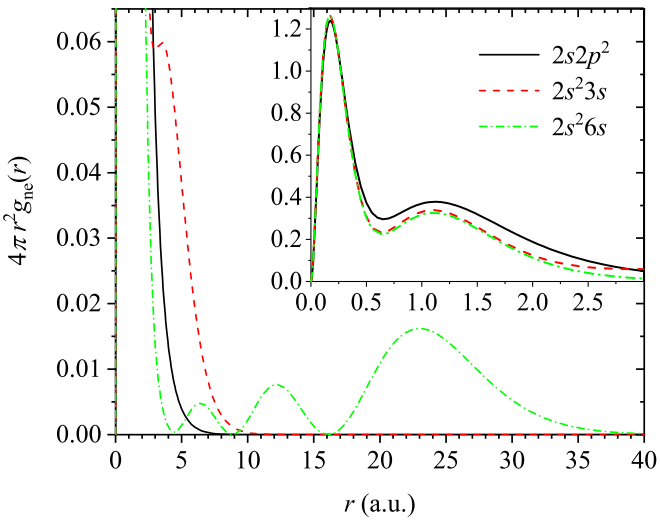

FIG. 1. Nucleus-electron correlation functions for the $1s^22s2p^2$, $1s^22s^23s$, and $1s^22s^26s$ states of $^{12}C^+$ ion. The same plots for $^{13}C^+$ and $^{14}C^+$ are virtually indistinguishable and are not shown here.

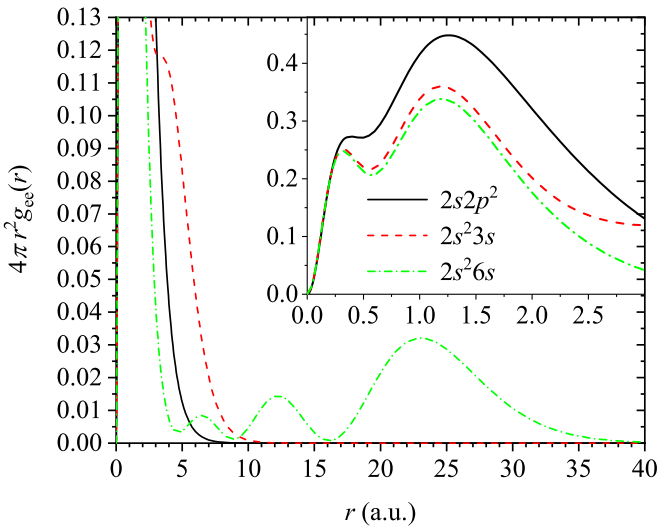

FIG. 2. Electron-electron correlation functions for the $1s^22s2p^2$, $1s^22s^23s$, and $1s^22s^26s$ states of $^{12}C^+$ ion. The same plots for $^{13}C^+$ and $^{14}C^+$ are virtually indistiguishable and are not shown here.

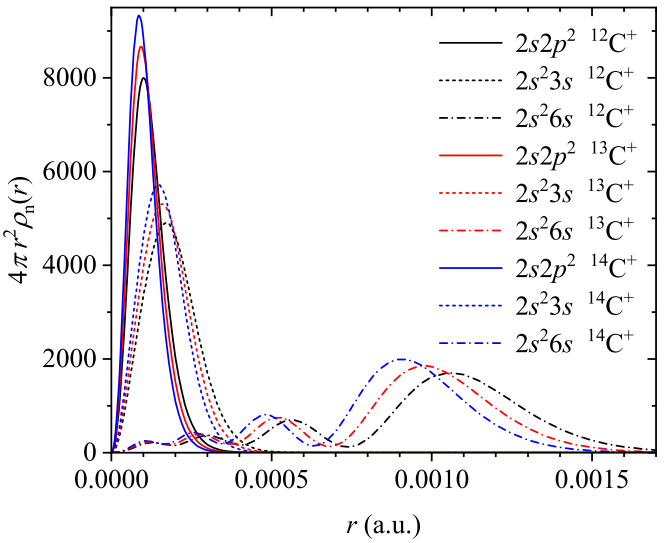

FIG. 3. The densities of the nucleus in the center-of-mass coordinate frame for the $1s^22s2p^2$, $1s^22s^23s$, and $1s^22s^26s$ states of C^+.

state and the $2s^26s$ state. The isotopic shift of $\langle r_i \rangle$ and $\langle r_{ij} \rangle$ for the former state is only $+0.000001$ and $+0.000003$ a.u., but it changes sign and becomes -0.000024 and -0.000044 a.u., respectively, for the latter state.

Lastly, we find it interesting to show plots comparing the nucleus–electron correlation functions calculated for different states of ^{12}C. In Fig. 1, a comparison of these functions is shown for states $2s2p^2$, $2s^23s$, and $2s^26s$. All correlation functions clearly show the electronic shell structure of the different states of the carbon cation with more maxima appearing for the higher $2s^26s$ state than for lowest two states. The shell structure of the electrons also manifests itself in the plots of the electron–electron correlations functions, which are presented in Fig. 2. The fact that the nucleus is treated on equal footing with the electrons in or calculations makes it possible to also look at its density distribution. The plots of the nuclear density (in the center-of-mass frame of reference) are presented in Fig. 3. In this figure the isotopic effect for the nuclear density is clearly visible. As one can expect, the nuclear density, regardless of the state, is much (4–5 orders of magnitude) more localized around the center of mass of the atom than the electronic density (make note of the scale of horizontal axis in Figs. 1 and 3). This reflects the fact that the nucleus is nearly fixed in space.

ACKNOWLEDGMENTS

This work has been supported by the Ministry of Education and Science of Kazakhstan via state-targeted program "Center of Excellence for Fundamental and Applied Physics" (Grant No. BR05236454), Nazarbayev University (faculty development Grant No. 090118FD5345), and the National Science Foundation (Grant No. 1856702).

[1] E. A. Hylleraas, Neue berechnung der energie des heliums im grundzustande, sowie des tiefsten terms von ortho-helium, Z. Phys. **54**, 347 (1929).

[2] W. H. Heitler and F. W. London, Wechselwirkung neutraler atome und homöopolare bindung nach der quantenmechanik, Z. Phys. **44**, 455 (1927).

[3] T. Kinoshita, Ground state of the helium atom, Phys. Rev. **105**, 1490 (1957).

[4] C. L. Pekeris, Ground state of two-electron atoms, Phys. Rev. **112**, 1649 (1958).

[5] G. W. F. Drake, M. M. Cassar, and R. A. Nistor, Ground-state energies for helium, h^- and ps^-, Phys. Rev. A **65**, 054501 (2002).

[6] C. Schwartz, Experiment and theory in computations of the he atom ground state, Int. J. Mod. Phys. E **15**, 877 (2006).

[7] C. Schwartz, Further computations of the he atom ground state, arXiv:math-ph/0605018.

[8] H. Nakashima and H. Nakatsuji, Solving the schrödinger equation for helium atom and its isoelectronic ions with the free iterative complement interaction (ici) method, J. Chem. Phys. **127**, 224104 (2007).

[9] V. A. Yerokhin and K. Pachucki, Theoretical energies of low-lying states of light helium-like ions, Phys. Rev. A **81**, 022507 (2010).

[10] D. T. Aznabaev, A. K. Bekbaev, and V. I. Korobov, Nonrelativistic energy levels of helium atoms, Phys. Rev. A **98**, 012510 (2018).

[11] M. Puchalski and K. Pachucki, Relativistic, QED, and finite nuclear mass corrections for low-lying states of li and Be^+, Phys. Rev. A **78**, 052511 (2008).

[12] J. S. Sims and S. A. Hagstrom, Hylleraas-configuration-interaction study of the 2^2s ground state of neutral lithium and the first five excited ^2s states, Phys. Rev. A **80**, 052507 (2009).

[13] L. M. Wang, C. Li, Z.-C. Yan, and G. W. F. Drake, Isotope shifts and transition frequencies for the s and p states of lithium: Bethe

logarithms and second-order relativistic recoil, Phys. Rev. A **95**, 032504 (2017).
[14] F. W. King, D. Quicker, and J. Langer, Compact wave functions for the beryllium isoelectronic series, Li^- to Ne^{6+}: A standard hylleraas approach, J. Chem. Phys. **134**, 124114 (2011).
[15] J. S. Sims and S. A. Hagstrom, Hylleraas-configuration-interaction nonrelativistic energies for the ^1s ground states of the beryllium isoelectronic sequence, J. Chem. Phys. **140**, 224312 (2014).
[16] Y. Suzuki and K. Varga, *Stochastic Variational Approach to Quantum-Mechanical Few-Body Problems*, Lecture Notes in Physics (Springer, Berlin, 1998).
[17] S. Bubin, M. Pavanello, W.-C. Tung, K. L. Sharkey, and L. Adamowicz, Born–oppenheimer and non-born–oppenheimer, atomic and molecular calculations with explicitly correlated gaussians, Chem. Rev. **113**, 36 (2013).
[18] J. Mitroy, S. Bubin, W. Horiuchi, Y. Suzuki, L. Adamowicz, W. Cencek, K. Szalewicz, J. Komasa, D. Blume, and K. Varga, Theory and application of explicitly correlated gaussians, Rev. Mod. Phys. **85**, 693 (2013).
[19] S. Bubin and L. Adamowicz, Accurate variational calculations of the ground $^2p^o(1s^22s^22p)$ and excited $^2s(1s^22s2p^2)$ and $^2p^o(1s^22s^23p)$ states of singly ionized carbon atom, J. Chem. Phys. **135**, 214104 (2011).
[20] M. Puchalski, K. Pachucki, and J. Komasa, Isotope shift in a beryllium atom, Phys. Rev. A **89**, 012506 (2014).
[21] S. Bubin and L. Adamowicz, Prediction of ^1p rydberg energy levels of beryllium based on calculations with explicitly correlated gaussians, J. Chem. Phys. **140**, 024301 (2014).
[22] M. Puchalski, J. Komasa, and K. Pachucki, Explicitly correlated wave function for a boron atom, Phys. Rev. A **92**, 062501 (2015).
[23] S. Bubin and L. Adamowicz, Lowest ^2s Electronic Excitations of the Boron Atom, Phys. Rev. Lett. **118**, 043001 (2017).
[24] I. Hornyák, L. Adamowicz, and S. Bubin, Ground and excited ^1s states of the beryllium atom, Phys. Rev. A **100**, 032504 (2019).
[25] K. L. Sharkey and L. Adamowicz, An algorithm for non-relativistic quantum-mechanical finite-nuclear-mass variational calculations of nitrogen atom in $l = 0$, $m = 0$ states using all-electrons explicitly correlated gaussian basis functions, J. Chem. Phys. **140**, 174112 (2014).
[26] J. G. Ingalls, R. A. Chamberlin, T. M. Bania, J. M. Jackson, A. P. Lane, and A. A. Stark, Atomic carbon in southern hemisphere high-latitude clouds, Astrophys. J. **479**, 296 (1997).
[27] U. J. Sofia, J. A. Cardelli, K. P. Guerin, and D. M. Meyer, Carbon in the diffuse interstellar medium, Astrophys. J. **482**, L105 (1997).
[28] C. D. Wilson, Atomic carbon emission from individual molecular clouds in m33, Astrophys. J. **487**, L49 (1997).
[29] W. E. C. J. van der Veen, P. J. Huggins, and H. E. Matthews, Atomic carbon in the circumstellar envelopes of evolved stars, Astrophys. J. **505**, 749 (1998).
[30] U. Amaldi and G. Kraft, Radiotherapy with beams of carbon ions, Rep. Prog. Phys. **68**, 1861 (2005).
[31] O. Jäkel, State of the art in hadron therapy, AIP Conf. Proc. **958**, 70 (2007).
[32] S. Bubin and L. Adamowicz, Computer program atom-molnonbo for performing calculations of ground and excited states of atoms and molecules without assuming the born–oppenheimer approximation using all-particle complex explicitly correlated gaussian functions, J. Chem. Phys. **152**, 204102 (2020).
[33] S. Bubin and L. Adamowicz, Matrix elements of n-particle explicitly correlated gaussian basis functions with complex exponential parameters, J. Chem. Phys. **124**, 224317 (2006).
[34] M. Hamermesh, *Group Theory and Its Application to Physical Problems* (Addison-Wesley, Reading, MA, 1962).
[35] R. Pauncz, *Spin Eigenfunctions* (Plenum, New York, 1979).
[36] M. Stanke and L. Adamowicz, Finite-nuclear-mass calculations of the leading relativistic corrections for atomic d states with all-electron explicitly correlated gaussian functions, Phys. Rev. A **100**, 042503 (2019).
[37] W. E. Caswell and G. P. Lepage, Effective lagrangians for bound state problems in QED, qCD, and other field theories, Phys. Lett. B **167**, 437 (1986).
[38] K. Pachucki, Effective hamiltonian approach to the bound state: Positronium hyperfine structure, Phys. Rev. A **56**, 297 (1997).
[39] H. A. Bethe and E. E. Salpeter, *Quantum Mechanics of One- and Two-Electron Atoms* (Plenum, New York, 1977).
[40] A. I. Akhiezer and V. B. Berestetskii, *Quantum Electrodynamics* (Wiley, New York, 1965).
[41] H. Araki, Quantum-electrodynamical corrections to energy-levels of helium, Prog. Theor. Phys. **17**, 619 (1957).
[42] J. Sucher, Energy levels of the two-electron atom to order α^3 ry; ionization energy of helium, Phys. Rev. **109**, 1010 (1958).
[43] P. K. Kabir and E. E. Salpeter, Radiative corrections to the ground-state energy of the helium atom, Phys. Rev. **108**, 1256 (1957).
[44] Z.-C. Yan and G. W. F. Drake, Relativistic and QED Energies in Lithium, Phys. Rev. Lett. **81**, 774 (1998).
[45] K. Pachucki, Simple derivation of helium lamb shift, J. Phys. B **31**, 5123 (1998).
[46] G. W. F. Drake and S. P. Goldman, Bethe logarithms for ps^-, h^-, and heliumlike atoms, Can. J. Phys. **77**, 835 (2000).
[47] Z.-C. Yan, W. Nörtershäuser, and G. W. F. Drake, High Precision Atomic Theory for Li and Be^+: QED Shifts and Isotope Shifts, Phys. Rev. Lett. **100**, 243002 (2008).
[48] S. Bubin, J. Komasa, M. Stanke, and L. Adamowicz, Isotope shifts of the $1s^22s^2(^1s_0) \rightarrow 1s^22p^2(^1s_0)$ transition in the doubly ionized carbon ion c^{2+}, Phys. Rev. A **81**, 052504 (2010).
[49] K. Pachucki and J. Komasa, Relativistic and QED Corrections for the Beryllium Atom, Phys. Rev. Lett. **92**, 213001 (2004).
[50] K. Pachucki, $\alpha^4 r$ corrections to singlet states of helium, Phys. Rev. A **74**, 022512 (2006).
[51] G. W. F. Drake and W. C. Martin, Ionization energies and quantum electrodynamic effects in the lower $1sns$ and $1snp$ levels of neutral helium (^{4}He I), Can. J. Phys. **76**, 679 (1998).
[52] A. M. Ermolaev, Lamb shift in heliumlike ions, Phys. Rev. A **8**, 1651 (1973).

[53] K. Pachucki and J. Sapirstein, Recoil corrections to the lamb shift in helium, J. Phys. B **33**, 455 (2000).

[54] Z.-C. Yan and G. W. F. Drake, Lithium transition energies and isotope shifts: QED recoil corrections, Phys. Rev. A **66**, 042504 (2002).

[55] T. Kato, On the eigenfunctions of many-particle systems in quantum mechanics, Commun. Pure Appl. Math. **10**, 151 (1957).

[56] R. J. Drachman, A new global operator for two-particle delta functions, J. Phys. B **14**, 2733 (1981).

[57] K. Pachucki, W. Cencek, and J. Komasa, On the acceleration of the convergence of singular operators in gaussian basis sets, J. Chem. Phys. **122**, 184101 (2005).

[58] P. J. Mohr, D. B. Newell, and B. N. Taylor, Codata recommended values of the fundamental physical constants: 2014, Rev. Mod. Phys. **88**, 035009 (2016).

[59] A. E. Kramida, Yu. Ralchenko, J. Reader, and NIST ASD Team, NIST Atomic Spectra Database (ver. 5.7.1), 2019, available at http://physics.nist.gov/asd.